Solar Energy Materials and Solar Cells 170 (2017) 120–126

Contents lists available at ScienceDirect

Solar Energy Materials and Solar Cells

journal homepage: www.elsevier.com/locate/solmat

A comprehensive study of electrochromic device with variable infrared emissivity based on polyaniline conducting polymer

Yanlong Tian[a], Xiang Zhang[a], Shuliang Dou[a], Leipeng Zhang[a], Hongming Zhang[b], Haiming Lv[a], Lili Wang[a], Jiupeng Zhao[b], Yao Li[a,*]

[a] Center for Composite Materials and Structure, Harbin Institute of Technology, Harbin 150001, PR China
[b] School of Chemistry and Chemical Engineering, Harbin Institute of Technology, Harbin 150001, PR China

ARTICLE INFO

Keywords:
Infrared
Electrochromic device
Emissivity
PANI

ABSTRACT

In this study, dodecylbenzene sulfonate acid (DBSA) doped-polyaniline (PANI) films were synthesized in situ on Au/porous flexible substrate by electrochemical deposition. The emissivity change ($\triangle\varepsilon$) data of PANI films show a reversal from positive to negative as the polymerization charge increases. This trend can be explained by using the Drude free electron theory and the Hagen-Rubens approximation at low frequency due to the pseudo-metallic behavior of conducting polymers. The DBSA doped-PANI film was used as an active layer to fabricate an infrared (IR) electrochromic device. The $\triangle\varepsilon$ of this IR electrochromic device was measured to be 0.183, 0.388, and 0.315 in the wavelength ranges of 3–5 μm, 8–12 μm, and 2.5–25 μm, respectively. IR thermal images visually obtained from an IR thermal imager suggest that the IR electrochromic device possesses regulating capacity of thermal radiation within the operating waveband of the instrument (7.5–14 μm). The IR electrochromic device developed in this work can be potentially used in IR camouflage for military and thermal control for satellite.

1. Introduction

Electrochromic materials have been widely studied in the past several decades for applications in optical displays, automobile mirrors and optical-modulated windows (smart windows) because of their ability to reversibly switch color under applied alternating voltages [1–5]. Apparently, these applications just involve optical properties of the material in the visible and near infrared (IR) regions. Actually electrochromic materials also possess the ability to modulate light in the mid-IR region, and thus can be used in dynamic thermal IR optical switches [6–8]. For example, the switchable and controllable IR signature variation of electrochromism can act as a military camouflage countermeasure against IR cameras or detectors for all armed forces components (land vehicles and tanks, air-craft, soldiers, *etc*). Moreover, electrochromism is also a “smart” technique for satellite thermal control to replace bulky and costly mechanical louvers, and traditional fixed emissivity (ε) thermal control coatings. The currently reported IR electrochromic materials include tungsten oxide (WO_3), poly (3,4-ethylenedioxythiophene) (PEDOT) and polyaniline (PANI) [9–15]. When compared to transition metal oxides, which have poor processability and low flexibility owing to brittle fracture, conducting polymers exhibit better prospects for practical applications due to their light weight, flexibility, ease of deposition, and processability.

As early as 1995, Chandrasekhar *et al.* reported the first IR electrochromic system based on conducting polymers with a significant and dynamic IR variation [16]. Then through a series of the optimization experiments, they obtained a flexible electrochromic device with reflection mode. This device used poly(anethosulfonate) doped-PANI deposited on a Au/porous substrate as the functional layer, and could adjust effectively ε varying from 0.32 to 0.79 [17]. More importantly, the device was tested by mounting it on an actual space craft (NASA's ST5 mission launched in 2003) to evaluate its thermal control efficiency [18]. Recently, they reported a new generation of flexible electrochromic device based on the integrated design of front electrode and back electrode [19]. The device exhibited current state-of-the-art $\triangle\varepsilon$ (> 0.5) due to superduper sustainability of multilayer architectures. Moreover, some special techniques (such as ionic liquid electrolyte and solar absorptance reduction-coating) greatly accelerated the practical progress of the electrochromic devices in thermal control for satellite. However, the macromolecular polymer dopant used is very costly even if the IR electrochromic performance of the polymeric matrix doped-PANI is found to be excellent. Following this original work, Li *et al.* studied the IR electrochromic property of sulfuric acid doped-PANI using Chandrasekhar's patented device design [20,21]. This inorganic

* Corresponding author.
E-mail address: yaoli@hit.edu.cn (Y. Li).

http://dx.doi.org/10.1016/j.solmat.2017.05.053
Received 7 March 2017; Received in revised form 22 April 2017; Accepted 21 May 2017
Available online 06 June 2017

acid doped PANI system exhibited a low performance with an average dynamic variation in ε values of ca. 0.24 in the 8–12 μm wavelength region, which is much smaller than that observed for poly(anethosulfonate) doped-PANI. In addition to the above flexible device design, a non-flexible IR device made from PANI with a camphor sulfonic acid (CSA) dopant has been reported by Topart [22], where the specular reflectance was regulated from 0.2 to 0.65 at 12 μm.

In view of the excellent performances described above, PANI should be an ideal IR electrochromic material. Therefore, it is necessary to carry out an in-depth study on the IR electrochromic mechanism of PANI. Chandrasekhar considered that the different IR transmittances of the overlying PANI layer under different oxidation states affected the reflection from the underlying Au layer, and consequently, the PANI-Au/substrate film showed different reflectance and ε values [17]. Li's study also demonstrated that the change in transmittance of the PANI layer under different potentials was the main factor affecting the ε value [21]. Although the above two studies illustrated that the change in transmittance resulted in the variation of ε, the detailed mechanism of this phenomenon is still not clear.

To address these problems, in this study, we report for the first time, the preparation of PANI films doped with a small molecular organic acid (dodecylbenzene sulfonate acid (DBSA)) by electrochemical deposition on Au/porous substrate, and the assembly of an IR electrochromic device. The device had a sandwich configuration using DBSA doped-PANI-Au/porous substrate films (DBSA doped-PANI porous film) as both working and counter electrodes. The device shows an improved $\triangle\varepsilon$ of 0.183, 0.388, and 0.315 in the wavelength ranges 3–5 μm, 8–12 μm and 2.5–25 μm, respectively. The IR electrochromic mechanism of the DBSA doped-PANI porous film has been discussed in detail. Surprisingly, the obtained $\triangle\varepsilon$ data reveal a reversal of the change in $\triangle\varepsilon$ from positive to negative as the polymerization charge increases. This result is not completely consistent with the results reported by Chandrasekhar and Li. The Drude free electron theory and Hagen–Rubens approximation at a low frequency are used to explain our observations.

2. Experimental section

2.1. Materials

Aniline (99.5%) was purchased from Acros and distilled under reduced pressure. A microporous substrate of nylon 66 with a pore size from 0.5 to 2 μm was obtained from Haining Zhenghao Filter Equipment Co. China. A 200-nm-thick Au layer was deposited on the nylon 66 porous substrate by thermal evaporation. Propylene carbonate (PC) and lithium perchlorate were received from Alfa. Poly(vinylidene fluoride-*co*-hexafluoropropylene) (P(VDF-HFP)) with an average molecular weight of ca. 400,000, poly(methyl methacrylate) (PMMA) with an average molecular weight of ca. 350,000, N,N-Dimethylformamide (DMF), and DBSA were obtained from Aldrich.

2.2. Preparation of DBSA doped-PANI porous films

DBSA doped-PANI porous films were prepared on the surfaces of Au/nylon 66 porous substrates (2 × 3 cm^2) in an aqueous solution of 0.1 M DBSA and 0.01 M aniline monomer by a galvanostatic method with a current density of 0.1 mA cm^{-2} and a polymerization charge of 3.0C. Ag/AgCl and Pt foil were used as the reference electrode and counter electrode, respectively. For comparison, DBSA doped-PANI porous films with different polymerization charges from 0.5C to 2.5C and 3.5C to 5.0C were also prepared under the same conditions by adjusting the polymerization time.

2.3. Device assembly

As illustrated in Fig. 1, a solid polymer electrolyte film was obtained by firstly adding P(VDF-HFP) and PMMA into DMF under continuous stirring at 70 °C to form a clear solution. The weight percentages of P(VDF-HFP), PMMA and DMF were 9%, 1% and 91%, respectively. After vigorously stirring for 30 min, the solution was transferred to a watch-glass and maintained at 60 °C to remove DMF. Subsequently, the P(VDF-HFP) porous film was immersed in a PC solution containing 1 M lithium perchlorate for 24 h to ensure the adsorption of PC-lithium perchlorate into the polymer framework. Finally, the solid polymer electrolyte film was dried in air for 6 h and cut into various shapes and sizes for use in further experiments. The PC-lithium perchlorate content in the solid polymer electrolyte film was about 20 wt% obtained by measuring the weight change of the P(VDF-HFP) porous film before and after adsorption. The ionic conductivity of the solid polymer electrolyte film was estimated to be ~ 1.42 × 10^{-5} S cm^{-1} using electrochemical impedance spectrum (Fig. S1).

A device with a sandwich configuration was assembled using the DBSA doped-PANI porous film as both front and back electrodes and the solid polymer electrolyte film as the middle layer between the two electrodes. Prior to device assembly, a 30-μm-thick IR-transparent protection layer of polyethylene (PE) was heat-bonded directly to the surface of the front electrode polymer to prevent the permeation of the electrolyte onto the surface of the PANI layer. After each layer was assembled together, the device was suffered transient heating at 100 °C by two rollers, providing heat and mechanical pressure simultaneously to make each layers adhere firmly.

2.4. Measurements

Cyclic voltammetry (CV) and chronoamperometry (CA) tests were carried out using an electrochemical workstation (CHI760D, Shanghai Chenhua Instruments, China). Electrochemical impedance spectrum was measured on the electrochemical workstation at open-circuited potential in the frequency range from 0.1 Hz to 1 MHz. Typically, the electrochemical measurements on the DBSA doped-PANI porous films were performed in a three-compartment system with an aqueous solution of 0.1 M DBSA as the electrolyte, Ag/AgCl as the reference electrode and a Pt foil as the counter electrode. For the device, the electrochemical tests were conducted in a system with a two-electrode configuration. Thermal images of the device were obtained using an IR thermal imager (TI450, Fluke) with a spectral range of 7.5–14 μm. Spectral emittance (2.5–25 μm) of the PANI films and the device were measured ex-situ and in-situ *via* reflection method on a VERTEX 70 (Bruker) FT-IR spectrometer with an A562 integrating sphere owing to the opaque nature of both the PANI film and the device. The value of ε can be calculated by weighting ($1 - R_{(\lambda)}$) (namely spectral emittance) with the black body spectrum for a particular wavelength and integrating over the entire measured wavelength range according to the following two equations [23,24] :

$$B_{(\lambda)} = \frac{c_1 \lambda^{-5}}{exp[c_2/(\lambda T)]-1} \quad (1)$$

$$\varepsilon = \frac{\int_{\lambda_{min}}^{\lambda_{max}} (1 - R(\lambda)) B(\lambda) d\lambda}{\int_{\lambda_{min}}^{\lambda_{max}} B(\lambda) d\lambda} \quad (2)$$

where c_1 is the first radiation constant (3.7418 × 10^8 W μm^4 m^{-2}), c_2 is the second radiation constant (1.4388 × 10^4 μm K), λ is the wavelength, and T is the temperature.

3. Results and discussions

CV measurements were performed (scan rate of 50 mV s^{-1} between −0.25 and 0.8 V) to determine the electrochemical performance of the DBSA doped-PANI porous film with varying polymerization charge. As displayed in Fig. 2, all the CV curves exhibit a pair of broad redox peaks corresponding to the transformation between a leucoemeraldine base

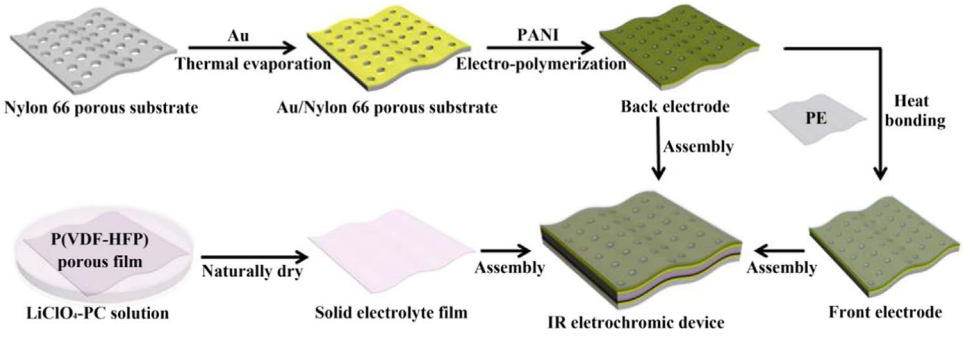

Fig. 1. A schematic illustration of the fabrication process for DBSA doped-PANI porous film and IR electrochromic device.

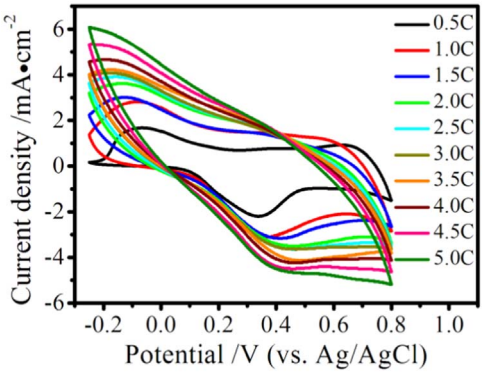

Fig. 2. CV curves of DBSA doped-PANI porous films with polymerization charges from 0.5C to 5.0C measured in an aqueous solution of 0.1 M DBSA with a scan rate of 50 mV s^{-1} between −0.25 and 0.8 V.

(LB) and an emeraldine salt (ES) [25,26]. Moreover, the oxidation peaks shift positively and the corresponding reduction peaks shift negatively with increase in the polymerization charge, which can be assigned to higher resistance of more PANI. Generally, IR electrochromic properties of the conductive polymers are directly related to their electrical conductivities [12,13,17–21]. Thus, the potentials of −0.25 V and 0.45 V were chosen to test the IR electrochromic performance of DBSA doped-PANI porous film because all the films completed state transformation between LB and ES at these two potentials.

Fig. 3 exhibits the emittance curves of DBSA doped-PANI porous films with different polymerization charges at potentials of −0.25 V and 0.45 V. The emittance curves at −0.25 V gradually rise with the increasing of polymerization charge. As for 0.45 V, the emittance curves first show a rising tendency from 0.5C to 2.5C, after which, a "plateau" is observed for further increasing the polymerization charge. The ε values of DBSA doped-PANI porous films prepared at different polymerization charges were calculated from the emittance curves using Eqs. (1) and (2), and the results are presented in Fig. 4 and Table 1. The ε values at −0.25 V and 0.45 V steadily increase when the polymerization charge is changed from 0.5C to 2.5C. When the polymerization charge exceeds 2.5C, the ε value at −0.25 V continues to increase up to 5.0C, whereas at 0.45 V, the ε value reaches a maximum, shows a plateau, and then starts to decrease at 3.5C.

The $\triangle\varepsilon$ values of DBSA doped-PANI porous films were also calculated and are listed in Table 1. The $\triangle\varepsilon$ values reveal a reversal from positive to negative as the polymerization charge increases. According to previous studies by Chandrasekhar and Li, the observed ε of a PANI-Au/porous substrate is integrated over the ε values of the overlying PANI layer and the underlying Au/porous substrate. The PANI layer appears to be substantially IR-transparent in the LB state, and thus, the PANI-Au/porous substrate has a low ε value owing to the strong reflecting effect of the Au layer. Conversely, the high IR absorption of the PANI layer in the ES state originating from bipolarons hinders the reflecting effect of the underlying Au layer, thus allowing the PANI-Au/porous substrate to have a high ε value [17,21]. Obviously, our observed $\triangle\varepsilon$ values from 0.5C to 3.0C are consistent with previous results, that is, the lowest ε is at the LB state, and the highest ε is at the ES state. However, when the polymerization charge reaches 3.5C, the LB state of PANI shows the highest ε, which is contrary to previously reported results.

Conducting polymers can exhibit a pseudo-metallic behavior; hence, their normal reflectance can be expressed according to the Drude free electron theory and the Hagen–Rubens approximation at a low frequency as follows [27–29]:

$$R(\omega) = 1 - (2\omega/\pi\sigma)^{1/2} \quad (3)$$

where R(ω) is the normal reflectance at the angular frequency ω, and σ is the electronic conductivity. It is noted that R(ω) is positively related to σ, and thus, the reflectance obtained by integrating R(ω) over the measured wavelength range is also positively related to σ. In general, the σ of PANI is closely related to its concentration of bipolarons, namely a higher concentration of bipolarons represents a higher σ. Therefore, ES state of PANI possesses a higher σ compared with LB state due to its higher concentration of bipolarons. This means that the reflectance of the PANI layer in the ES state is higher than that in the LB state. At the same time, the higher bipolaron concentration in the ES state also results in higher IR absorbance. Therefore, the IR transmittance of the PANI layer in the ES state should be lower than that in the LB state as the sum of the absorbance, the reflectance and the transmittance is 1. Smaller IR transmittance means a larger ε in accordance with the previous research result of Chandrasekhar and Li. However, the IR transmittances of the PANI layer in both ES and LB states gradually decrease to zero with increasing polymerization charge. It is easy to understand that the thickness of the PANI layer increases with increase in polymerization charge. The IR absorption of the PANI layer, as well as the dopant-induced free carriers will also increase, leading to a decrease in the IR transmittance of the PANI layer. When the IR transmittance of the PANI layer is zero, the ε value of DBSA doped-PANI porous film depends only on the PANI layer. According to Kirchhoff's law of thermal radiation, a material's frequency-dependent emittance is equal to its frequency-dependent absorbance in thermal equilibrium. In the entire measured wavelength range, ε can be defined as [30,31]:

$$\varepsilon = 1 - R \quad (4)$$

In this case, as the PANI layer in the ES state has a higher reflectance owing to its better electric conductivity, the ε of the PANI layer in the ES state will become lower than that at the LB state, which is in agreement with our observed result when the polymerization charge is changed from 3.5C to 5.0C.

In fact, the IR transmittance change of the PANI layer caused by increasing the polymerization charge is not synchronous in the whole wavelength range (2.5–25 μm). As shown in Fig. 3e, the emittance of the PANI layer with a polymerization charge of 2.5C in the LB state is larger than that in the ES state only in certain regions of the spectrum (8.4–9.0 μm, 9.6–9.7 μm and 9.8–9.9 μm). This clearly indicates that the IR transmittance of the PANI layer with 2.5C is zero in these small wavebands. Subsequently, with further increase in the polymerization

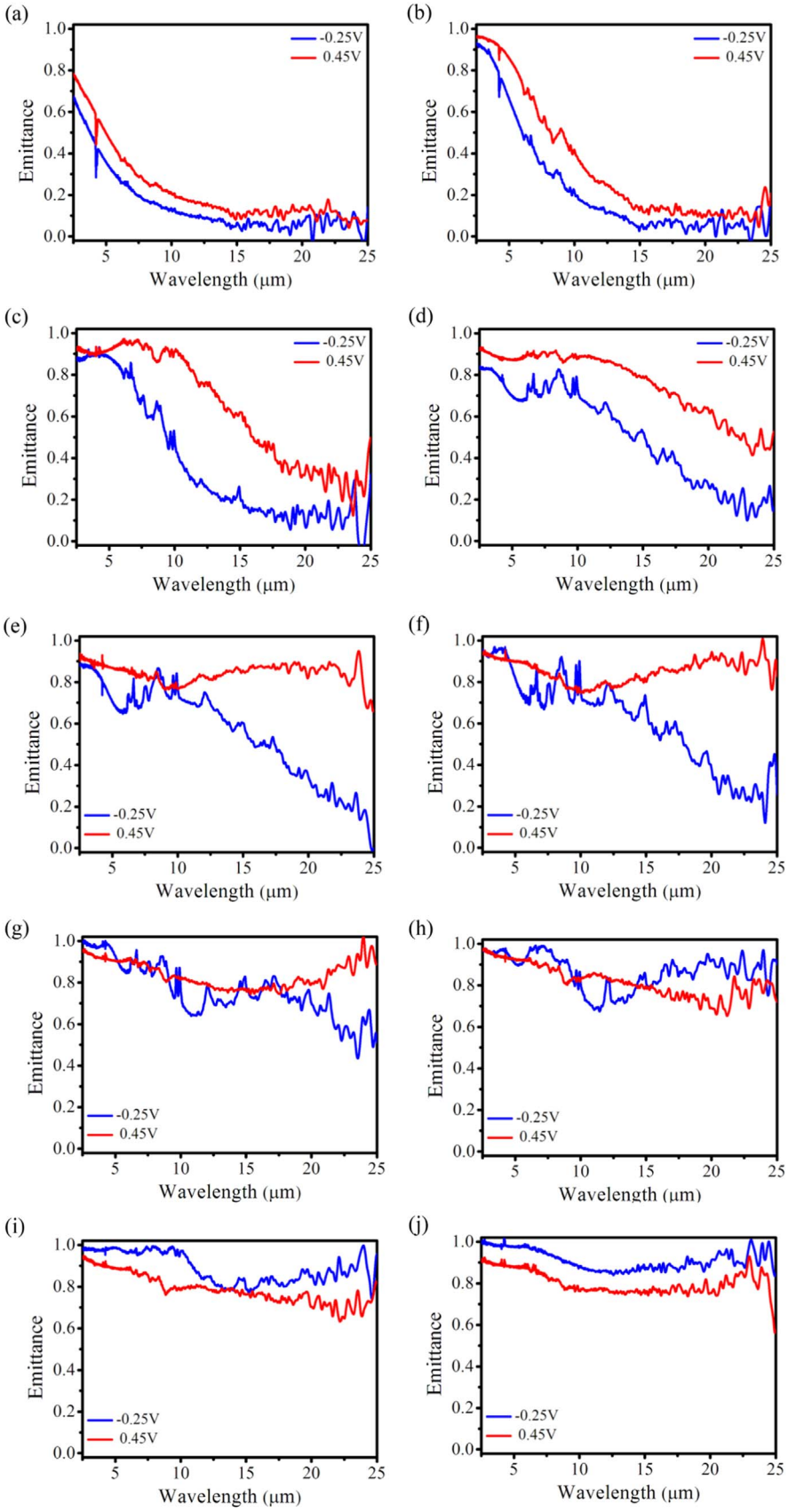

Fig. 3. Emittance curves of DBSA doped-PANI porous films with different polymerization charges of (a) 0.5C, (b) 1.0C, (c) 1.5C, (d) 2.0C, (e) 2.5C, (f) 3.0C, (g) 3.5C, (h) 4.0C, (i) 4.5C, and (j) 5.0C at −0.25 V and 0.45 V.

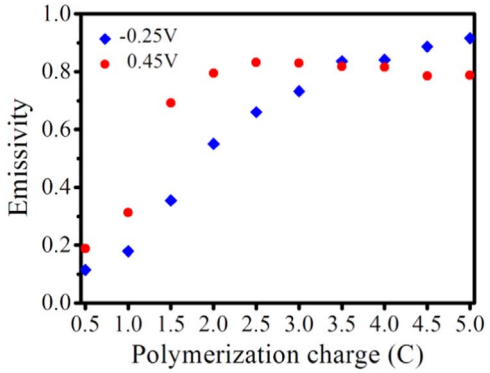

Fig. 4. ε data of DBSA doped-PANI porous films as a function of the polymerization charge in the range 0.5C to 5.0C at −0.25 V and 0.45 V.

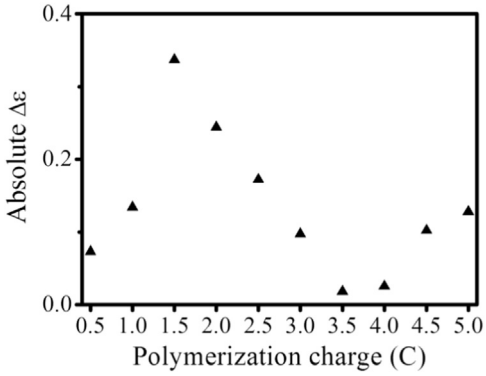

Fig. 5. Absolute △ε of DBSA doped-PANI porous films as a function of the polymerization charge in the range of 0.5C to 5.0C.

charge, a relatively higher emittance in the LB state appears in more and more spectral wavebands. Finally, the IR transmittance of the PANI layer becomes IR-opaque at 5.0C in the entire wavelength range of 2.5–25 μm.

Furthermore, we obtained a similar result by altering the polymerization current density (Fig. S2 and Table S1). When the current density reaches 0.2 mA cm^{-2}, the △ε values also display a reverse change from positive to negative as the polymerization charge increases. However, this reverse change from a current density of 0.2 mA cm^{-2} occurs for 3.0C, which is prior to 3.5C with a current density 0.1 mA cm^{-2}. This "beforehand phenomenon" is attributed to the greater growth rate of the electro-polymerization process at 0.2 mA cm^{-2}.

Fig. 5 presents the absolute △ε evolution of DBSA doped-PANI porous films with increasing polymerization charges. By combination of Fig. 3 and 5, the evolution of absolute △ε can be divided into three stages. Firstly, IR transmittance of PANI layer is not equal to zero in the entire wavelength range of 2.5–25 μm when the polymerization charge is less than 2.5C. The values of absolute △ε undergo a changing process of increase first and then decrease. According to the above description, the changes in transmittance of the PANI layer between two different potentials are responsible for the absolute △ε values of DBSA doped-PANI porous films. When the polymerization charge is lower (between 0.5C and 1.0C) or is higher (> 2.0C), the transmittance changes between the two different potentials are also insufficient for providing a larger absolute △ε. Thus, the optimum polymerization charge to obtain the greatest transmittance change and the highest absolute △ε value of 0.337 is 1.5C. In the second stage, IR transmittance of PANI layer is not equal to zero only in partial wavelength range when the polymerization charge is less than 5.0C. In this case, absolute △ε is an integrated △ε value because the emittance in the LB state is larger than that in the ES state in the opaque wavelength range (denoted as band A) and the emittance in the ES state is larger than that in the LB state in the other wavelength range (denoted as band B). When the polymerization charge is between 2.5C and 3.0C, the absolute $\triangle\varepsilon_{bandB}$ value is dominant and gradually reduces, leading to the decrease of the absolute △ε value. When the polymerization charge is between 3.5C and 4.5C, the absolute $\triangle\varepsilon_{bandA}$ value is dominant and gradually increases with the increasing of polymerization charges, leading to the increase of the absolute △ε value. In the third stage, IR transmittances of PANI layer is equal to zero in the entire wavelength range of 2.5–25 μm when the polymerization charge is 5.0C. The absolute △ε value is determined by the reflectance change of PANI layer between two different potentials. Moreover, it should be noted that the absolute △ε value of 0.337 at 1.5C is much larger than that of 0.128 at 5.0C, which indicates that strong reflecting effect of the underlying Au layer is very critical for obtaining high absolute △ε value of DBSA doped-PANI porous film.

IR electrochromic device can be used in IR camouflage for military and thermal control for satellite to tune radiation energy [6–8]. In order to demonstrate the practicability of the DBSA doped-PANI porous film for variable emissivity applications, a DBSA doped-PANI porous film with polymerization charge of 1.5C was used to assemble the IR electrochromic device with a sandwich construction. Digital photographs of the device in the voltage range between −1.5 V and 0.5 V can be found in the supporting video (Video S1 (right)). Notably, the color of the IR electrochromic device can change reversibly from grass-green to yellow with a change in voltage. The yellow color at −1.5 V is from the Au layer owing to the almost transparent nature of PANI in the LB state. The grass-green color is due to the presence of ES, which implies that ES is formed at 0.5 V.

Fig. 6 exhibits the emittance curves of the IR electrochromic device at different voltages. These curves present a steadily rising trend as the applied voltage is increased. The large, intense, and extremely narrow IR absorptions at 3.5 μm, 6.8 μm and 14 μm are due to the absorbance of protection layer PE. The ε values of the device are also calculated from the emittance curves in the wavelength ranges of 3–5 μm, 8–12 μm, and 2.5–25 μm versus the applied voltage. The results are shown in Fig. 7 and Table 2. When PANI is in the LB state (namely −1.5 V), it is most IR-transparent, and thus leads to the emittance curve having the lowest intensity due to the strong reflecting effect of the Au under layer. When PANI is in the ES state (namely 0.5 V), it has the lowest IR transmittance and results in the highest emittance curve. The other voltages represent the transformation from the LB state to the ES state, thus leading to a rising trend in the emittance curves. The evolution of ε in the wavelength range of 8–12 μm and 2.5–25 μm shows a similar tendency, that is, ε gradually increases as the applied voltage is increased. The tendency of evolution of ε in the 3–5 μm range differs slightly from those in the 8–12 μm and 2.5–25 μm ranges. In this case, ε declines slightly once the applied voltage exceeds −0.2 V. △ε values of the device are calculated to be 0.183, 0.388, and 0.315 in the

Table 1
The △ε data of DBSA doped-PANI porous films with different polymerization charges from 0.5C to 5.0C.

	0.5 C	1.0 C	1.5 C	2.0 C	2.5 C	3.0 C	3.5 C	4.0 C	4.5 C	5.0 C
$\varepsilon_{-0.25V}$	0.115	0.179	0.355	0.551	0.660	0.733	0.836	0.841	0.887	0.916
$\varepsilon_{0.45V}$	0.188	0.313	0.692	0.795	0.832	0.830	0.818	0.816	0.785	0.788
$\triangle\varepsilon^a$	0.073	0.134	0.337	0.244	0.172	0.097	−0.018	−0.025	−0.102	−0.128

[a] $\triangle\varepsilon = \varepsilon_{0.45\ V} - \varepsilon_{-0.25\ V}$.

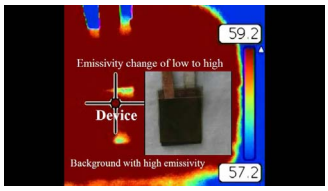

Video S1. Digital photograph and IR thermal image of the IR electrochromic device at different voltage. Supplementary material related to this article can be found online at http://dx.doi.org/10.1016/j.solmat.2017.05.053.

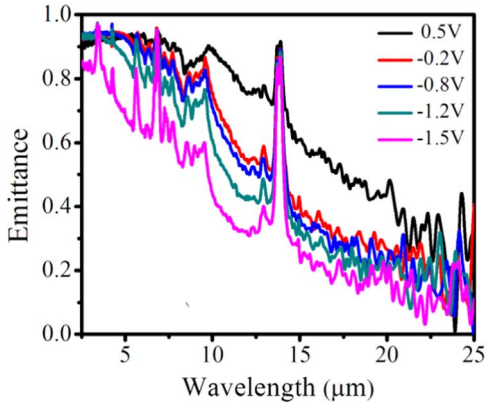

Fig. 6. Emittance curves of the IR electrochromic device at different voltages.

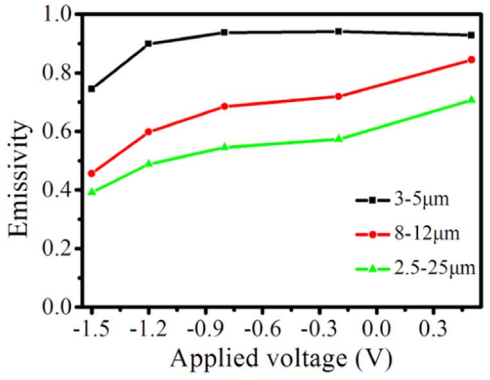

Fig. 7. The evolution of ε in the wavelength ranges of 3–5 μm, 8–12 μm and 2.5–25 μm versus applied voltage.

Table 2
The △ε data of the IR electrochromic device in different wavebands.

	3–5 μm	8–12 μm	2.5–25 μm
$\varepsilon_{-1.5\ V}$	0.745	0.456	0.391
$\varepsilon_{-1.2\ V}$	0.898	0.598	0.488
$\varepsilon_{-0.8\ V}$	0.937	0.685	0.545
$\varepsilon_{-0.2\ V}$	0.941	0.719	0.573
$\varepsilon_{0.5V}$	0.928	0.844	0.706
$\triangle\varepsilon^{a}$	0.183	0.388	0.315

[a] $\triangle\varepsilon = \varepsilon_{0.5\ V} - \varepsilon_{-1.5\ V}$.

wavelength ranges of 3–5 μm, 8–12 μm, and 2.5–25 μm, respectively. This ε data indicates that our IR electrochromic device can modulate light in both 3–5 μm and 8–12 μm regions. In particular, the △ε of 0.388 in 8–12 μm is much larger than that (0.24) previously reported for sulfuric acid doped-PANI device [20].

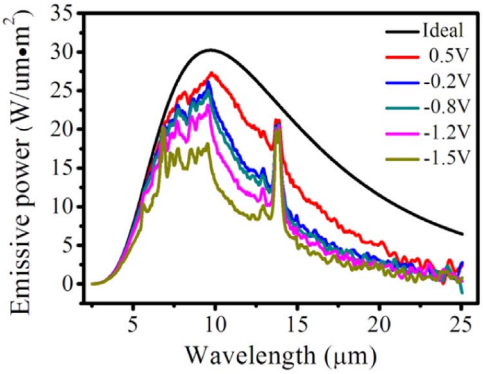

Fig. 8. Emission curves of the IR electrochromic device at different voltage.

The emission results of the IR electrochromic device at different voltages obtained from Eq. (2), as well as the corresponding ideal black body spectra (298.15 K) are presented in Fig. 8. The ideal black body spectrum is a slightly asymmetric bell shaped curve with a long wavelength tail. Compared to the ideal black body spectrum, all the emission spectra of the device exhibit a completely asymmetric shape with a rough line style. As expected, the emission spectra of the device at different voltages show distinctly different integral areas, suggesting that the device has a thermal radiation regulating capacity. The results apparently indicate that our IR electrochromic device can modulate light in the whole range 2.5–25 μm region, particularly in the 3–5 μm and 8–12 μm regions. Furthermore, in order to visually illustrate the thermal radiation modulating capacity the IR electrochromic device, an IR thermal image was obtained using the IR thermal imager (Video S1 (left)). The temperatures of two different states respectively were 60.1 °C and 57.5 °C, while the background was 55.6 °C. In IR thermal images, a higher temperature represents a higher state of radiation. Indeed, ours IR electrochromic device exhibits two different colors of red and blue, clearly pointing to the modulating capacity of thermal radiation of our device in the operating waveband of the instrument (7.5–14 μm).

4. Conclusions

In summary, DBSA doped-PANI films have been prepared at different polymerization charges *via* the electro-polymerization of aniline on the surfaces of Au/porous substrates. The change in ε of the DBSA doped-PANI porous film is closely related to the change in transmittance of the PANI layer under different potentials and thicknesses. The obtained IR electrochromic device assembled from DBSA doped-PANI films has a variable emissivity with △ε of ~ 0.183 in the 3–5 μm, 0.388 in 8–12 μm, and 0.315 in the 2.5–25 μm ranges of wavelength. The present IR electrochromic device has considerable potential for applications in military camouflage and thermal control of satellites.

Acknowledgements

We thank National Natural Science Foundation of China (No. 51572058, 51174063, 51502057), the Natural Science Foundation of Heilongjiang Province (E201436), the International Science & Technology Cooperation Program of China (2013DFR10630, 2015DFE52770), Specialized Research Fund for the Doctoral Program of Higher Education (SRFDP 20132302110031) and the Fundamental Research Funds for the Central Universities (No. HIT.MKSTISP.201628).

Appendix A. Supplementary material

Supplementary data associated with this article can be found in the online version at http://dx.doi.org/10.1016/j.solmat.2017.05.053.

References

[1] K. Nakamura, K. Kanazawa, N. Kobayashi, Electrochemical luminescence modulation in a Eu(III) complex-modified TiO_2 electrode, J. Mater. Chem. C 3 (2015) 7135–7142.

[2] H. Lv, N. Li, H. Zhang, Y. Tian, H. Zhang, X. Zhang, H. Qu, C. Liu, C. Jia, J. Zhao, Y. Li, Transferable TiO_2 nanotubes membranes formed via anodization and their application in transparent electrochromism, Sol. Energy Mater. Sol. Cells 150 (2016) 57–64.

[3] S. Tsuneyasu, L. Jin, K. Nakamura, N. Kobayashi, An electrochemically-driven dual-mode display device with both reflective and emissive modes using poly(*p*-phenylenevinylene) derivatives, Jpn. J. Appl. Phys. 55 (2016) 041601.

[4] Z. Tong, H. Yang, N. Li, H. Qu, X. Zhang, J. Zhao, Y. Li, Versatile displays based on a 3-dimensionally ordered macroporous vanadium oxide film for advanced electrochromic devices, J. Mater. Chem. C 3 (2015) 3159–3166.

[5] G. Cai, J. Tu, D. Zhou, X. Wang, C. Gu, Growth of vertically aligned hierarchical WO_3 nano-architecture arrays on transparent conducting substrates with outstanding electrochromic performance, Sol. Energy Mater. Sol. Cells 124 (2014) 103–110.

[6] C. Nilsson, E.H. Karlsson, H. Kariis, Polymer based devices with adaptable infrared reflection and transmission, Proceedings of SPIE 6192 6192U, 2006.

[7] B. Kim, J.K. Koh, J. Park, C. Ahn, J. Ahn, J.H. Kim, S. Jeon, Patternable PEDOT nanofilms with grid electrodes for transparent electrochromic devices targeting thermal camouflage, Nano Converg. 2 (2015) 19.

[8] I. Schwendeman, J. Hwang, D.M. Welsh, D.B. Tanner, J.R. Reynolds, Combined visible and infrared electrochromism using dual polymer devices, Adv. Mater. 13 (2001) 634–637.

[9] A. Bessiere, L. Beluze, M. Morcrette, B. Viana, Optical properties of an all-plastic $WO_3{\cdot}H_2O$-based infrared modulator, J. Appl. Phys. 95 (2001) 7701–7706.

[10] Y. Huang, Y. Zhang, X. Zeng, X. Hu, Study on Raman spectra of electrochromic c-WO_3 films and their infrared emittance modulation characteristics, Appl. Surf. Sci. 202 (2002) 104–109.

[11] A. Larsson, G. Niklasson, Infrared emittance modulation of all-thin-film electrochromic devices, Mater. Lett. 58 (2004) 2517–2520.

[12] C. Louet, S. Cantin, J. Dudon, P. Aubert, F. Vidal, C. Chevrot, A comprehensive study of infrared reflectivity of poly(3,4-ethylene-dioxythiophene) model layers with different morphologies and conductivities, Sol. Energy Mater. Sol. Cells 143 (2015) 141–151.

[13] L. Goujon, P. Aubert, L. Sauques, F. Vidal, D. Teyssié, C. Chevrot, Soft and flexible Interpenetrating Polymer Networks hosting electroreflective poly(3,4-ethylene-dioxythiophene), Sol. Energy Mater. Sol. Cells 127 (2014) 33–42.

[14] P. Chandrasekhar, B.J. Zay, S. Barbolt, R. Werner, G.C. Birur, A. Paris, High Performance Variable Emittance Devices for Spacecraft Application Based on Conducting Polymers Coupled with Ionic Liquids, AIP Conference Proceedings 1103, 2009, pp. 101–104.

[15] P. Chandrasekhar, B.J. Zay, S. Barbolt, R. Werner, E. Caldwell, Variable Emittance Skins for Active Thermal Control in Spacecraft Based on Conducting Polymers, Ionic Liquids and Specialized Coatings, AIP Conference Proceedings 1208, 2010, pp. 99–104.

[16] P. Chandcasekhar, T.J. Dooley, FarIR transparency and dynamic infrared signature control with novel conducting polymer systems, Proc. SPIE 2528 (1995) 169–180.

[17] P. Chandrasekhar, B.J. Zay, G.C. Birur, S. Rawal, E.A. Pierson, L. Kauder, T. Swanson, Large, switchable electrochromism in the visible through far-infrared in conducting polymer devices, Adv. Funct. Mater. 12 (2002) 95–103.

[18] P. Chandrasekhar, B.J. Zay, T. McQueeney, A. Scara, S. Ross, G.C. Birur, S. Haapanen, L. Kauder, T. Swanson, D. Douglas, Conducting polymer (CP) infrared electrochromics in spacecraft thermal control and military applications, Synth. Met. 135–136 (2003) 23–24.

[19] P. Chandrasekhar, B.J. Zay, D. Lawrence, E. Caldwell, R. Sheth, R. Stephan, J. Cornwell, Variable-emittance infrared electrochromic skins combining unique conducting polymers, ionic liquid electrolytes, microporous polymer membranes, and semiconductor/polymer coatings, for spacecraft thermal control, J. Appl. Polym. Sci. 131 (2014) 5829–5836.

[20] H. Li, K. Xie, Y. Pan, M. Yao, C. Xin, Variable emissivity infrared electrochromic device based on polyaniline conducting polymer, Synth. Met. 159 (2009) 1386–1388.

[21] H. Li, K. Xie, Y. Pan, H. Wang, H. Wang, Study of the mechanism of the variable emissivity infrared electrochromic device based on polyaniline conducting polymer, Synth. Met. 162 (2012) 22–25.

[22] P. Topart, P. Hourquebie, Infrared switching electroemissive devices based on highly conducting polymers, Thin Solid Films 352 (1999) 243–248.

[23] H. Demiryont, K.C. ShannonIII, Variable Emittance Electrochromic Devices for Satellite Thermal Control, AIP Conference Proceedings 880, 2007, pp. 51–58.

[24] B.V. Bergeron, K.C. White, J.L. Boehme, A.H. Gelb, P.B. Joshi, Variable absorptance and emittance devices for thermal control, J. Phys. Chem. C 112 (2008) 832–838.

[25] D. Ge, L. Yang, Z. Tong, Y. Ding, W. Xin, J. Zhao, Y. Li, Ion diffusion and optical switching performance of 3D Ordered nanostructured polyaniline films for advanced electrochemical/electrochromic devices, Electrochim. Acta 104 (2013) 191–197.

[26] L. Zhao, L. Zhao, Y. Xu, T. Qiu, L. Zhi, G. Shi, Polyaniline electrochromic devices with transparent graphene electrodes, Electrochim. Acta 55 (2009) 491–497.

[27] K. Lee, E.K. Miller, A.N. Aleshin, R. Menon, A.J. Heeger, J.H. Kim, C. Oh Yoon, H. Lee, Nature of the metallic state in conducting polypyrrole, Adv. Mater. 10 (1998) 456–459.

[28] F.A. Modine, D.Y. Smith, Approximate formulas for the amplitude and the phase of the infrared reflectance of a conductor, J. Opt. Soc. Am. A 1 (1984) 1171–1174.

[29] J. Joo, E.J. Oh, G. Mm, A.G. MacDiarmid, A.J. Epsteina, Evolution of the conducting state of polyaniline from localized to mesoscopic metallic to intrinsic metallic regimes, Synth. Met. 69 (1995) 251–254.

[30] J.A. Schuller, T. Taubner, M.L. Brongersma, Optical antenna thermal emitters, Nat. Photon. 3 (2009) 658–661.

[31] J.W. Salisbury, A. Wald, D.M. D'Aria, Thermal-infrared remote sensing and Kirchhoff's law: 1. Laboratory measurements, J. Geophys. Res. 99 (1994) 11897–11911.